

## Control the Crosslinking of Epoxy-asphalt via Induction Heating

Apostolidis, Panos; Liu, Xueyan; van de Ven, Martin; Erkens, Sandra; Scarpas, Athanasios

**DOI**

[10.1080/10298436.2019.1652741](https://doi.org/10.1080/10298436.2019.1652741)

**Publication date**

2019

**Document Version**

Final published version

**Published in**

International Journal of Pavement Engineering

**Citation (APA)**

Apostolidis, P., Liu, X., van de Ven, M., Erkens, S., & Scarpas, A. (2019). Control the Crosslinking of Epoxy-asphalt via Induction Heating. *International Journal of Pavement Engineering*, 21 (2020)(8), 956-965. <https://doi.org/10.1080/10298436.2019.1652741>

**Important note**

To cite this publication, please use the final published version (if applicable). Please check the document version above.

**Copyright**

Other than for strictly personal use, it is not permitted to download, forward or distribute the text or part of it, without the consent of the author(s) and/or copyright holder(s), unless the work is under an open content license such as Creative Commons.

**Takedown policy**

Please contact us and provide details if you believe this document breaches copyrights. We will remove access to the work immediately and investigate your claim.



## Control the crosslinking of epoxy-asphalt via induction heating

Panos Apostolidis, Xueyan Liu, Martin van de Ven, Sandra Erkens & Tom Scarpas

To cite this article: Panos Apostolidis, Xueyan Liu, Martin van de Ven, Sandra Erkens & Tom Scarpas (2020) Control the crosslinking of epoxy-asphalt via induction heating, International Journal of Pavement Engineering, 21:8, 956-965, DOI: [10.1080/10298436.2019.1652741](https://doi.org/10.1080/10298436.2019.1652741)

To link to this article: <https://doi.org/10.1080/10298436.2019.1652741>



© 2019 The Author(s). Published by Informa UK Limited, trading as Taylor & Francis Group



Published online: 16 Aug 2019.



Submit your article to this journal [↗](#)



Article views: 743



View related articles [↗](#)





View Crossmark data [↗](#)



Citing articles: 3 View citing articles [↗](#)

## Control the crosslinking of epoxy-asphalt via induction heating

Panos Apostolidis <sup>a</sup>, Xueyan Liu<sup>a</sup>, Martin van de Ven<sup>a</sup>, Sandra Erkens <sup>a</sup> and Tom Scarpas<sup>a,b</sup>

<sup>a</sup>Section of Pavement Engineering, Faculty of Civil Engineering and Geosciences, Delft University of Technology, Delft, Netherlands; <sup>b</sup>Department of Civil Infrastructure and Environmental Engineering, Khalifa University of Science and Technology, Abu Dhabi, United Arab Emirates

### ABSTRACT

Induction heating driven polymerisation is an in-situ curing technique for epoxy-asphalt systems that maintains most of the advantages of temperature-driven polymerisation and it solves the need for longer curing time periods at lower temperatures before traffic can be allowed. In particular, induction heating can be utilised to accelerate the polymerisation of paving mixes with a thermo-hardening nature. In this study, steel fibres are dispersed in a mix and during exposure to an alternating electro-magnetic field generated by induction coils, they are heated leading to the rapid initiation of epoxy-asphalt polymerisation. This research presents the implementation of a finite element model analysis for assessing the potential of utilising steel fibres for the development of inductive mixes with sufficient induction heating efficiency. A produced and compacted mix with steel fibres was reconstructed by means of CT scans on samples from the mix and its effective electrical conductivity was calculated. Also, the electro-magnetic induction-driven polymerisation of epoxy-asphalt is simulated by extending a model developed elsewhere. The extended method can be used to predict the evolution of the curing process, and further of mechanical properties thereby indicating that electro-magnetic induction represents a reliable polymerisation method to cure epoxy-asphalt systems.

### ARTICLE HISTORY

Received 9 July 2019  
Accepted 1 August 2019

### KEYWORDS

Induction heating; epoxy-asphalt; polymerisation; finite element method

## Introduction

Pavement construction and maintenance are large energy consumers worldwide, and thus improving the current practices in terms of energy efficiency will support the worldwide effort for achieving sustainable development. However, besides improving the environmental footprint of paving industry, also attention needs to be given to the cost because the cost to construct, rehabilitate and maintain the pavement infrastructure has become dramatically high recently (Highway Statistics 2016). Therefore, even small improvements in pavement-related technologies can lead to substantial public cost savings. Within this framework, road authorities, contractors and material suppliers have started to explore new technologies to minimise the energy footprint of pavements and to leverage the economic benefits by developing eco-friendly solutions. One of these technologies is the electro-magnetic induction for heating the asphalt paving materials for improving healing (Garcia *et al.* 2009, Liu *et al.* 2013, Apostolidis *et al.* 2016) and compaction (Bueno *et al.* 2018, Zhou *et al.* 2018). However, asphalt mixes, which are the most commonly used materials in the pavement industry, are non-inductive. For this reason, inductive particles, mostly steel fibres, are added in the mixes to make them sensitive for electro-magnetic induction. Especially, asphaltic mixes with steel fibres can be made sensitive to electro-magnetic induction under a time-variable magnetic field applied by an induction coil. The magnetic field induces eddy currents in the fibres in the mortar phase (i.e. the binding part between stone particles) of the asphalt mix according to

Faraday's law. Based on Joule's law, the electric current flows generate heat in the steel fibres (a material with high electrical conductivity) and consequently to the binder in the mortar via heat conduction.

Due to the increasing demands for longer-lasting paving materials, polymer modification in asphalt mixes has become an attractive solution. Among other polymer modifiers, epoxy-based polymers have captured the interest of road network administrations as an importance modification technique to change the chemistry of asphalt binders specially designed for critical pavement applications, such as orthotropic steel deck bridges and airfields (Simpson *et al.* 1960, Burns 1964, Balala 1969). The epoxy modifiers in asphalt binder differ from the conventional thermoplastic block copolymers, such as styrene-butadiene styrene (SBS), due to the fact that once the reactive epoxy is fully cured in asphalt, a thermosetting system is created with limited possibilities to be re-melted. However, a remarkable durability improvement has been observed when epoxy-based polymers were blended with asphalt binders offering a new binder type with improved durability (i.e. increased oxidative aging resistance) (Herrington and Alabaster 2008, Apostolidis *et al.* 2019a) and increased affinity with steel surfaces (Jia *et al.* 2014, Chen *et al.* 2018). Also, the incorporation of epoxy-based polymers in asphaltic materials for surfacing paving solutions has resulted in mixes with enhanced lifespan (Widyatmoko *et al.* 2006, Herrington and Alabaster 2008, Luo *et al.* 2015, Wu *et al.* 2017).

While the epoxy modification in asphalt has been introduced as a high-performance solution on high deflection bridges since the 1970s (San Mateo-Hayward Bridge in 1967 and San Francisco-Oakland Bay Bridge in 1969) (Lu and Bors 2015), recent studies have suggested the industrial transfer of this technology to roadway pavements under the OECD project (International Transport Forum 2017). The two primary concerns that delay the implementation of this technology are the high initial cost of an epoxy-based modifier and the uncontrolled temperature-driven irreversible curing (i.e. polymerisation) of newly developed paving mixes. Contractors could face high risks of construction failures, because of the relatively slow curing of epoxy-asphalt (EA) systems in case of allowing too early traffic after construction (International Transport Forum 2017).

The proposed technology in this paper describes a technique based on electro-magnetic induction heating which can be used to control the reactions of EA systems with steel fibres. This technology will provide a solution to pavements to be opened to traffic immediately after construction. Via this technology, the problem of uncontrolled hardening can be overcome and this will make the widespread use of epoxy-based modifiers in paving materials possible. However, there is no evidence available to indicate that electro-magnetic induction can be used to assist the in-situ curing of EAs.

### Induction heating-driven polymerisation

The curing of EAs due to the crosslinking of epoxy pre-polymers and the network formation is a process that involves the continuous chemical alteration with the assistance of a hardener. In addition to hardener, the initiation of epoxy modifier crosslinking in asphalt is triggered via external heating. However, no heating-driven curing techniques are available to enable in-situ polymerisation of EA systems. Issues like too slow reaction and limited polymerisation can occur when the EA systems have no access to external heat sources especially when construction takes place at low temperatures, which will become standard practice in the near future.

In this study, the application of induction heating technique is proposed to overcome the temperature restrictions during field operations and to control in-situ polymerisation. Induction heating as an assisting curing technology has not been tried before in EA systems, however, it can be used as an external heating method to trigger indirectly the epoxy polymerisation. The added steel fibres are the only included components in the asphaltic matrix responding to the supplied alternating magnetic field and they operate as individual heat generators within the EAs since they are able to be induced by alternating magnetic fields, causing temperature and reaction rate gradients.

### Incorporation of steel fibres

To illustrate the impact of incorporating steel fibres to develop inductive systems able to be cured via induction heating, a three-dimensional finite element (FE) mesh is generated by using X-ray computed tomography (CT) (two-dimensional) scans by means of a specialised image processing tool, called

SIMPLEWARE. X-ray CT technique is completely non-destructive and used for obtaining digital information of features in the interior of opaque objects, in this case, steel fibres in asphalt mortar.

For realistic analyses, high-resolution X-ray CT scans were obtained from a real sample prepared in the laboratory by mixing steel fibres with asphalt mortar (i.e. the asphaltic part between aggregate particles made by binder, filler and fine sand particles). The weight percentage of components in asphalt mortar was 28:38:34 for asphalt binder, filler and fine sand. Steel fibres (7756 kg/m<sup>3</sup>, length 2.5 mm and diameter 0.083 mm) were mixed with the before mentioned components following a laboratory preparation method described elsewhere (Apostolidis *et al.* 2016).

In SIMPLEWARE, two voxels of interest were selected using the grey scale threshold to segment steel fibres in asphalt mortar. Here, the asphalt mortar part was considered as one phase and the second phase was the randomly distributed steel fibres. Quantitative information was obtained as well regarding the volume fraction of fibres in mortar (4.7% of the total volume).

The typical laboratory measuring method of the electrical conductivity is the two-probe with the digital multi-meter, mostly used for materials with relatively high electrical conductivity (>10 × 10<sup>-7</sup> S/m). In particular, two electrodes supplied with electric potential are placed in contact with the two opposite sides of a sample and based on the potential difference between the electrodes measurements are obtained (Figure 1).

Theoretically, the governing equation when the two-probe measurements are taking place is the charge conservation law as described in Equation (1)

$$\frac{\partial \rho}{\partial t} + \nabla \cdot \mathbf{J} = 0 \quad (1)$$

where  $\rho$  is the charge density,  $t$  is time and  $\mathbf{J}$  is the current density vector.

The current density vector can be described by using Ohm's law in Equation (2)

$$\mathbf{J} = \sigma \cdot \mathbf{E} = -\sigma \nabla V \quad (2)$$

where  $\sigma$  is the electrical conductivity,  $\mathbf{E}$  is the electric field and  $V$  is the electric potential.

A potential gradient is applied at opposite sides of the specimen and the current density vector is calculated. The total current that runs through the sample can be calculated by integration over a cross-section the projection of the current density on the area. This is done in Equation (3)

$$I = \iint_A (\mathbf{J} \cdot \hat{n}) dA \quad (3)$$

where  $I$  is the total current that runs through the specimen,  $dA$  is an elementary area over which the current density is applied and  $\hat{n}$  is the normal vector to that area. The specimen is then viewed as an equivalent resistor in an electric circuit as explained in Figure 1 and its resistance is calculated in Equation (4)

$$R = \frac{V}{I} \quad (4)$$

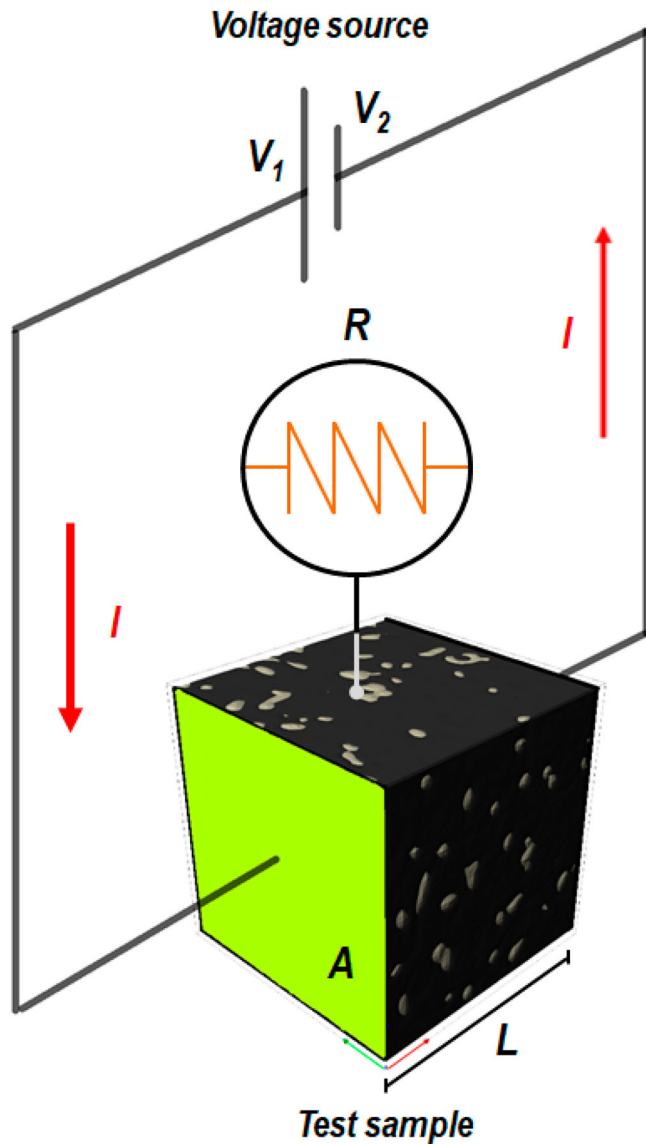


**Figure 1.** Schematic of electrical conductivity measurements in inductive EA system.

where  $R$  is the equivalent resistance of the specimen and  $V$  is the electric potential difference acting on the opposite sides.

As the specimen is a rectangular parallelepiped, the electrical resistance of the specimen is proportional to its resistivity, its length and inversely proportional to its cross-sectional area. These relationships yield Equation (5)

$$R = \rho_{b,\text{eff}} \frac{L}{A} \quad (5)$$

where  $\rho_{b,\text{eff}}$  is the effective bulk resistivity,  $A$  is the cross-sectional area and  $L$  is the length of the specimen. The effective bulk conductivity is calculated in Equation (6)

$$\sigma_{b,\text{eff}} = \frac{1}{\rho_{b,\text{eff}}} \quad (6)$$

where  $\sigma_{b,\text{eff}}$  is the effective bulk conductivity.

To determine the effective electrical conductivity of the studied material, the generated mesh of an inductive asphalt

mix described before was imported into the COMSOL Multiphysics. The mesh geometry is a cube with length of 1.18 mm that contains  $502 \times 10^3$  elements and  $2.285 \times 10^3$  degrees of freedom and it is presented in Figure 2(a). The fibres distribution and their connectivity in the studied geometry is demonstrated in Figure 2(b). For the purpose of this analysis, it is necessary to define the properties of the individual components of the studied composite. The electrical conductivity magnitudes of asphaltic and steel part were considered to be  $10 \times 10^{-6}$  and  $4.8 \times 10^6$  (ASM International Materials Properties Database Committee 2000), respectively. An electric potential gradient of 10 V is applied between the two opposite sides (Figure 2(c)), whereas the remaining four sides are considered as electric insulation. A side acting as electric insulation is translated to a zero normal component of the current density vector on that side.

The current density vector is solved for and the total current is calculated by means of Equation (3). Using Equations (4–6) the effective bulk conductivity for the inductive asphalt  $\sigma_{b,\text{eff, st}} = 0.89552$  S/m is calculated. Comparing with the electrical conductivity of steel fibres, it seems that the asphalt part – with electrical conductivity several orders of magnitude lower – is the limiting factor. The iso-surface plot of the electrical potential is presented in Figure 3(a), whereas the current density vector in asphalt part and in the inductive fibres is plotted in Figure 3(b,c), respectively.

Specifically, the electric potential spatial distribution in the material is demonstrated in Figure 3(a) which in terms of magnitude leads to higher current densities on the randomly oriented fibres (Figure 3(c)). From Figure 3 (b,c), it is apparent that the magnitude of current density in the asphaltic part is definitely lower than of fibres due to the enormous conductivity difference. From these images, the impact of inclusion of high electrical conductivity values, herein the steel fibres but also others such as steel slag (Apostolidis *et al.* 2017, Apostolidis 2018b), on the effective conductivity of the whole composite system is significant. Furthermore, the latter is influenced by the amount of inclusions in the matrix as well since the high volumes of the added inclusions come in contact with each other creating conductive pathways in the matrix. Hence, the material can pass the percolation threshold and can perform as conductor able to be induced by alternating magnetic fields.

### Crosslinking of epoxy-asphalt systems

Once the epoxy resin reacts chemically with the hardener in asphalt, irreversible polymerisation is initiated by crosslinking a three-dimensional polymeric network. The reaction rate of EA systems is temperature-dependent and the conversion (degree of cure) is initiated via thermal heating (Apostolidis *et al.* 2018a, 2019b). Hence, the ability of the EA system to be cured in-situ within sufficient time at very low-temperature conditions during and after construction can be improved. Based on this technology, a model of in-situ polymerisation triggered by electro-magnetic induction was developed to predict the evolution of conversion of crosslinking EAs.



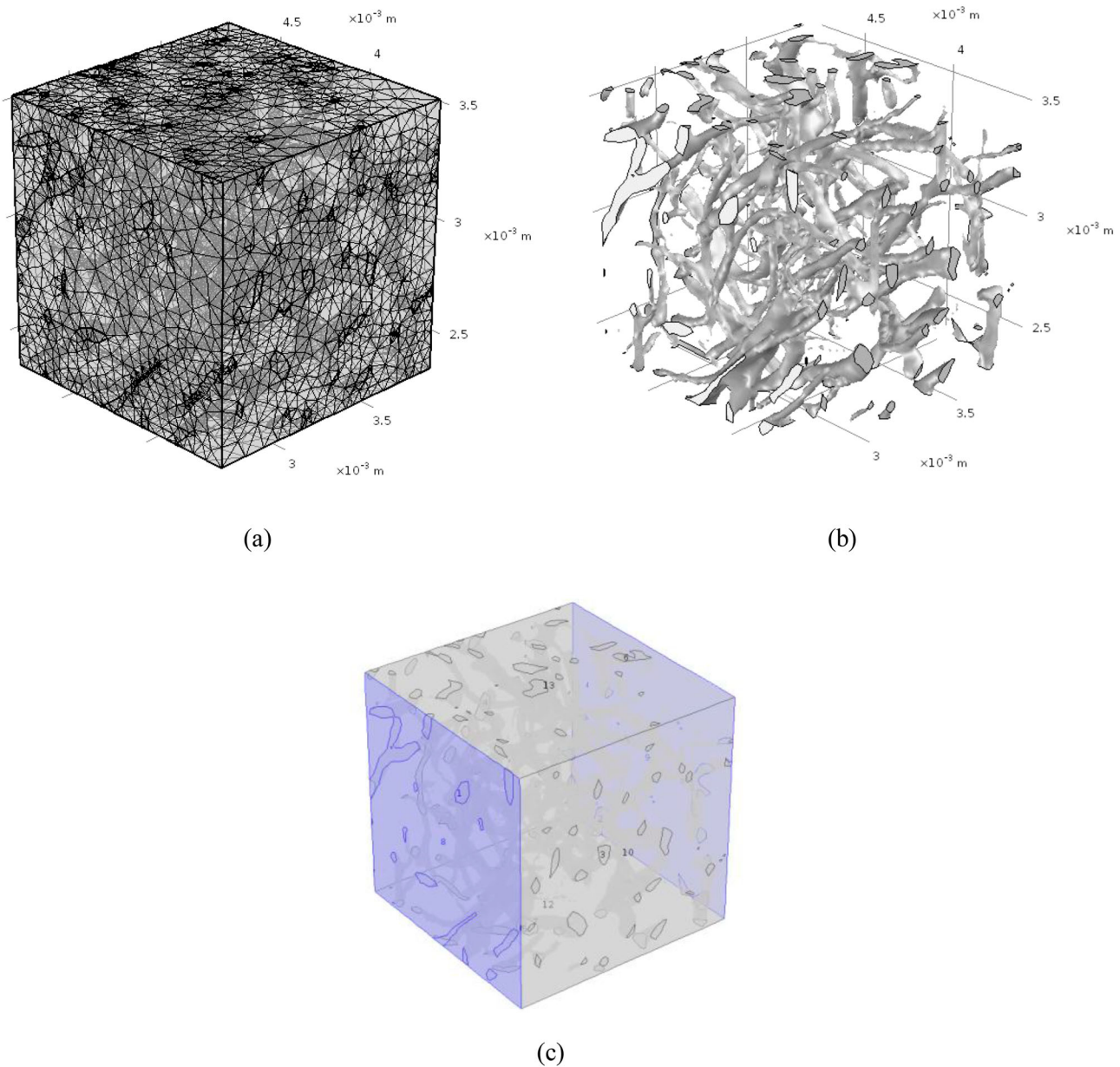


**Figure 2.** Inductive EA system; (a) finite element mesh reconstructed by CT-scans, (b) steel fibres distribution, and (c) the opposite sides between which the potential difference is applied.

The determination of the predicted level of conversion via induction is crucial since the evolution of material properties of an EA, such as glass transition temperature, viscosity and modulus, depends on the level of conversion (Apostolidis *et al.* 2018a, 2019b). Herein, the reaction process is considered as one step  $n^{\text{th}}$  order exothermic reaction and the kinetics model before the material gelation is given as

$$\frac{\partial x}{\partial t} = A_f \exp\left(-\frac{E_a}{RT}\right) \cdot (1-x)^n \quad (7)$$

where  $x$  is the conversion [1],  $A_f$  is the pre-exponential kinetic factor (i.e. reaction rate) [1/s],  $E_a$  is the activation energy [kJ/mol],  $R$  is the universal gas constant [1] and  $n$  is the reaction order of polymerisation [1]. Both  $E_a$  and  $A_f$  parameters are related with the chemistry of incorporating epoxy-based polymers and govern the reactivity and subsequently the

crosslinking performance of epoxy-asphalt systems. In the past, very fast reacting epoxy resins have been developed of  $5 \times 10^3$  1/s reaction rate and 40 kJ/mol activation energy (Yang *et al.* 1999, Prime *et al.* 2005). In previous studies on the thermodynamics of epoxy-asphalt systems, the activation energy of pure epoxy and epoxy-asphalt binders was determined from 50 and 80 kJ/mol, and from 46 and 65 kJ/mol, respectively (Yin *et al.* 2014, Li *et al.* 2014).

The initiation of the polymerisation process is driven by external heat and, for this reason, the use of induction heating is so important. The governing equation of the transient heat conduction within the crosslinking EA is described as

$$\rho c_p \mathbf{u} \cdot \nabla T - \nabla \cdot (k \nabla T) = \rho \Delta H_{\text{exo}} \frac{\partial x}{\partial t} \quad (8)$$

where  $\rho$  is the mass density of the EA system,  $k$  denotes the

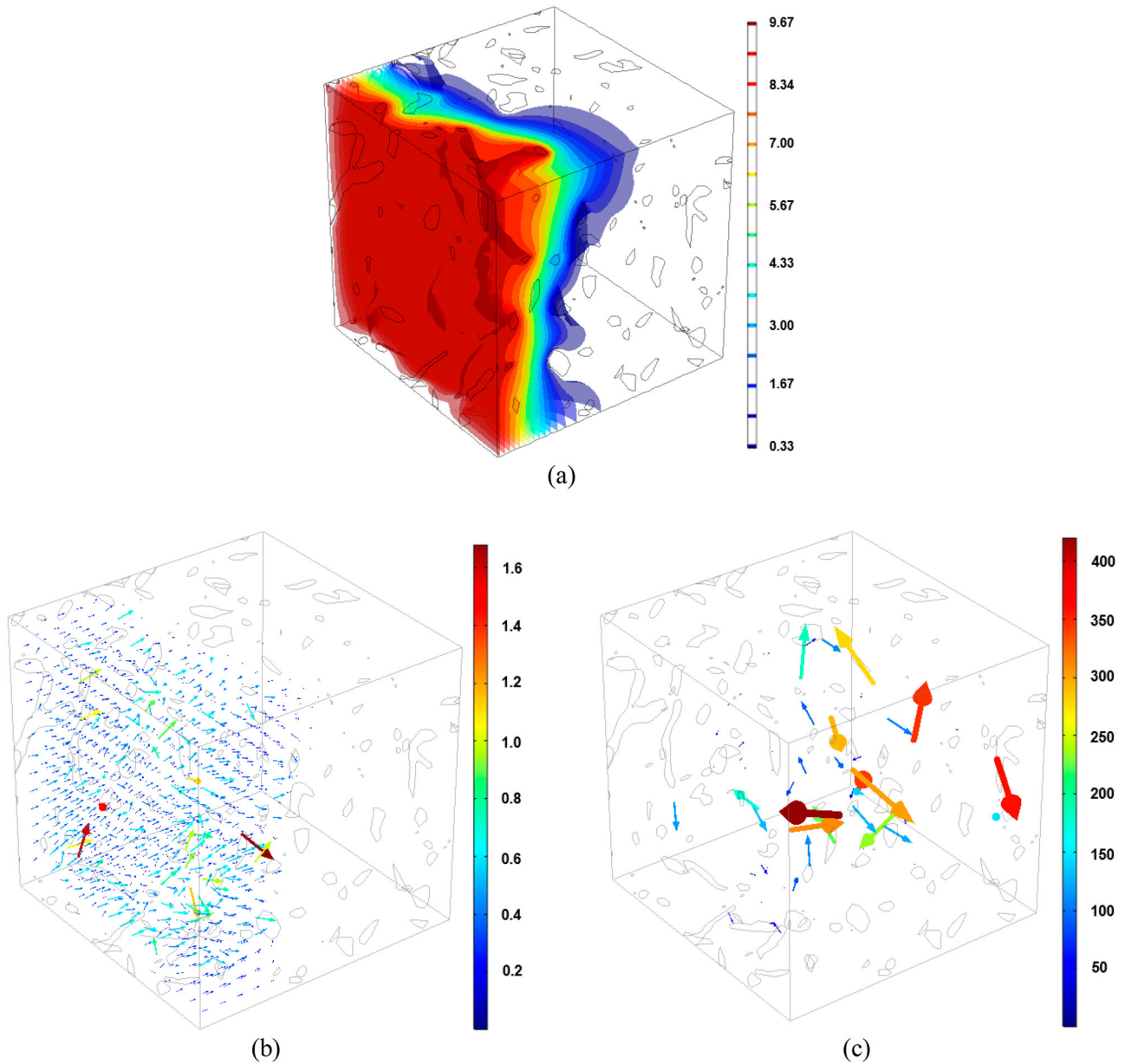


**Figure 3.** (a) Iso-surface of electric potential [V], (b) current density vector in asphaltic part [A/m<sup>2</sup>], and (c) current density vector in steel fibres [A/m<sup>2</sup>].

thermal conductivity,  $c_p$  is the heat capacity,  $\mathbf{u}$  is the travelling speed of electro-magnetic source (i.e. induction coils),  $T$  is the temperature,  $\Delta H_{exo}$  is the polymerisation enthalpy (kW/m<sup>3</sup>). As epoxy turns into a networked microstructure, heat is released, which is proportional to the consumption rate of reactive elements in the EA system.

The impact of convection and radiation heat on the energy balance of the system is formulated as

$$\mathbf{n} \cdot k\nabla T = h \cdot (T_{sur} - T) \quad (9)$$

where  $h$  is the overall convective thermal coefficient and  $T_{sur}$  denotes the surrounding temperature, the initial temperature was 20°C.

The thermal diffusion on the top surface of studied medium (i.e. inductive pavement) is described as

$$\mathbf{n} \cdot k\nabla T = \sigma \cdot em(T_{amb}^4 - T^4) \quad (10)$$

in which  $T_{amb}$  is ambient air temperature 20°C,  $\sigma$  is the Stefan–Boltzmann constant of  $5.67 \times 10^{-8} \text{ W/m}^2\text{K}^4$ ,  $\mathbf{n}$  is the normal vector and  $em$  is the surface emissivity of 0.5. More details about the governing equations of induction heating and coupling electro-magnetic and heat transfer phenomena can be found in (Apostolidis *et al.* 2017).

In case of thermosets, the material transformation takes place when the thermosetting resin is liquid with low molecular weight and transforms to a rigid solid of infinite polymeric network without any molecular movement. This transformation happens when the gel point is reached. Extensive research has been conducted to determine the appropriate models to simulate the time-dependent chemo-mechanical performance of EA systems before and after the gelation (Apostolidis *et al.* 2018a, 2019b). In this paper, emphasis is given on the efficiency of electro-magnetic induction as heating method to drive the material polymerisation interpreted by the evolution of conversion.

### Finite element simulations

The current multi-physics model is an extended version of an elsewhere developed model (Apostolidis *et al.* 2017) to simulate the induction heat generation and the temperature

development in asphalt pavements. In other words, the model can predict the heat development in a homogeneous continuum medium/pavement induced by an alternating electro-magnetic field. In this study, the source of the alternating

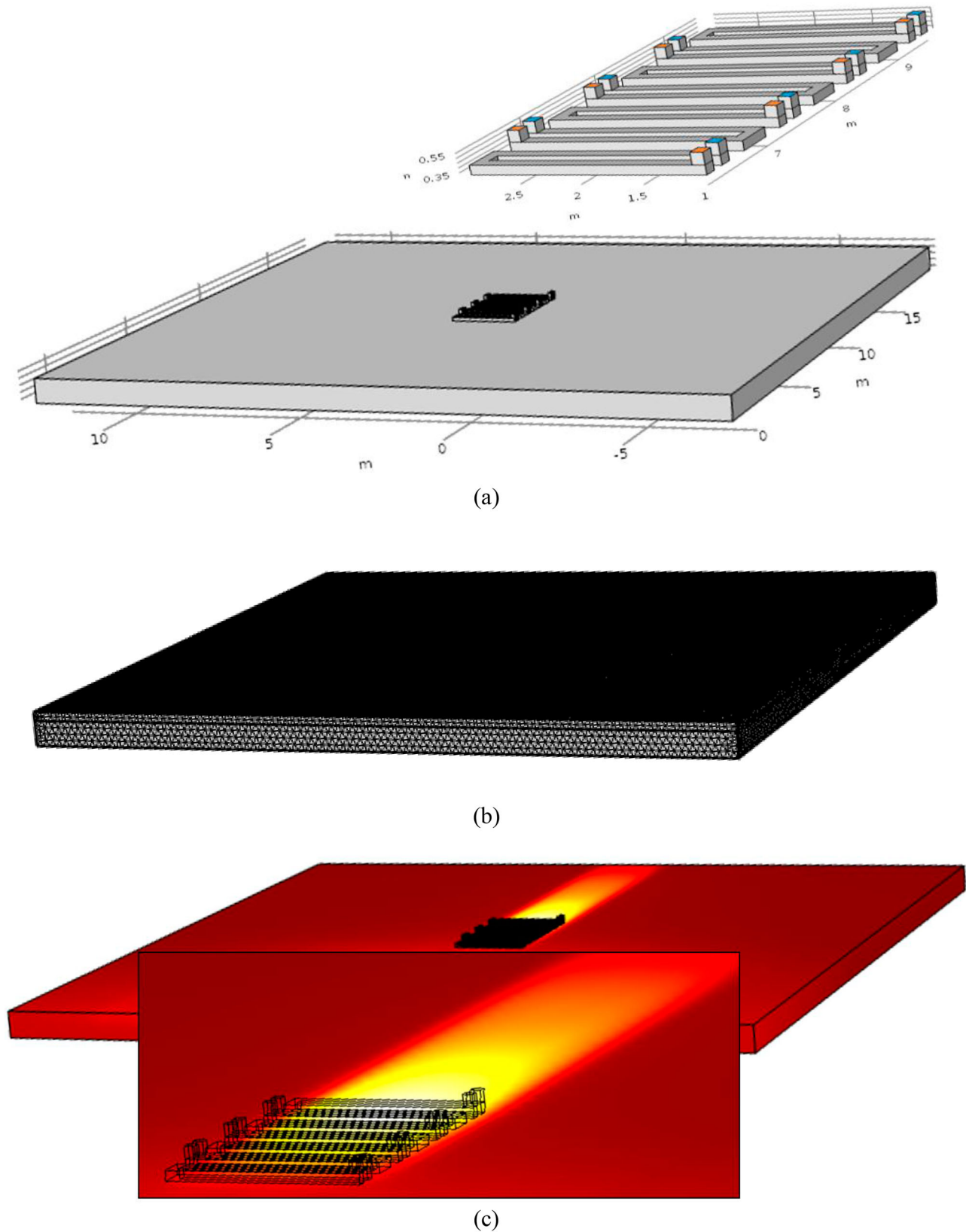


**Figure 4.** Studied model; (a) geometry (b) mesh, and (c) and heat generation due to electro-magnetic induction



field is a system of moving single-turn induction coils (see Figure 4(a)) along the medium. The incorporated domains for realising the current three-dimensional model were discretised by  $688 \times 10^3$  tetrahedral elements (see Figure 4(b)). Since a sensitivity analysis has been performed in the before mentioned research (Apostolidis *et al.* 2016) to study the impact of various operational and material parameters of induction heating systems, one configuration of induction parameters is selected for the current analysis.

The continuum medium is assumed to be a pavement structure (0.3 m height) of isotropic properties. The values of the effective properties of the whole medium/pavement were considered to be 1 [1] and 6 [1] for the relative magnetic permeability and electrical permittivity, respectively (Apostolidis *et al.* 2016). Taking into account the value of effective electrical conductivity obtained in the earlier section, the order of magnitude of electrical conductivity of the inductive medium was 1 S/m in agreement with a previous study (Apostolidis *et al.* 2017). In this study, the effective electrical conductivity selected was 10 S/m. The thermal conductivity and heat capacity were considered 0.2 W/(mK) and 1000 J/(kgK), respectively, as determined experimentally by (Apostolidis *et al.* 2016). These thermal properties have been used in both induction heating analyses in asphalt (Apostolidis *et al.* 2017) and heat transfer studies in epoxy-asphalt systems (Apostolidis *et al.* 2018a, 2019b). Copper was the selected material for the induction coils ( $6 \times 10^7$  S/m). The operational conditions of the prototype coils (Figure 4(a)) were 2 kV supplied power, 70 kHz frequency and travelling speed 0.01 m/s. The distance of coils with the surface of the top layer was 0.025 m and the horizontal distance between the single-turn coils was 0.2 m.

The generated heat pattern on the surface of the pavement by the moving induction coils (five single-tern coils) after 1000 s is shown in Figure 4(c). The herein predicted heat pattern coincides with another study on induction heating performance of asphalt mixes with moving coils (Bueno *et al.* 2018). In Apostolidis *et al.* 2017, the highest temperature on the surface of the medium was concentrated close to the coil's gates. In that research, although the effective electrical conductivity of the medium was based on laboratory tests, it was made clear that it is difficult to simulate heterogeneous materials (e.g. like these mixes), as being homogeneous, especially when the field fluxes (i.e. magnetic and subsequently heat) are concentrated locally around the inductive particles (steel fibres) in the mix.

The temperature development on the surface and the temperature gradient distribution within the medium is shown in Figure 5. It is apparent that the induction system is able to generate high temperatures on the surface of the medium (maximum surface temperature of 101.7°C), and it also generates sufficient propagation of the temperature gradient (iso-surface contours) inside the structure. Nevertheless, it is important to notice that the maximum surface temperature generated from induction and thus the heating efficiency of the current method is a function of the travelling speed of the induction coils over the surface. By increase of travelling speed of induction coils, increase of heating efficiency is achieved. The desired travelling speed for an efficient induction system at industrial-scale should be at least 1 m/s ( $\sim 3.6$  km/h, which is about the speed of a conventional paving/compaction process). However, the ultimate goal of the current analyses was to simulate the impact of the induction technology on the crosslinking of EAs. Figure 5

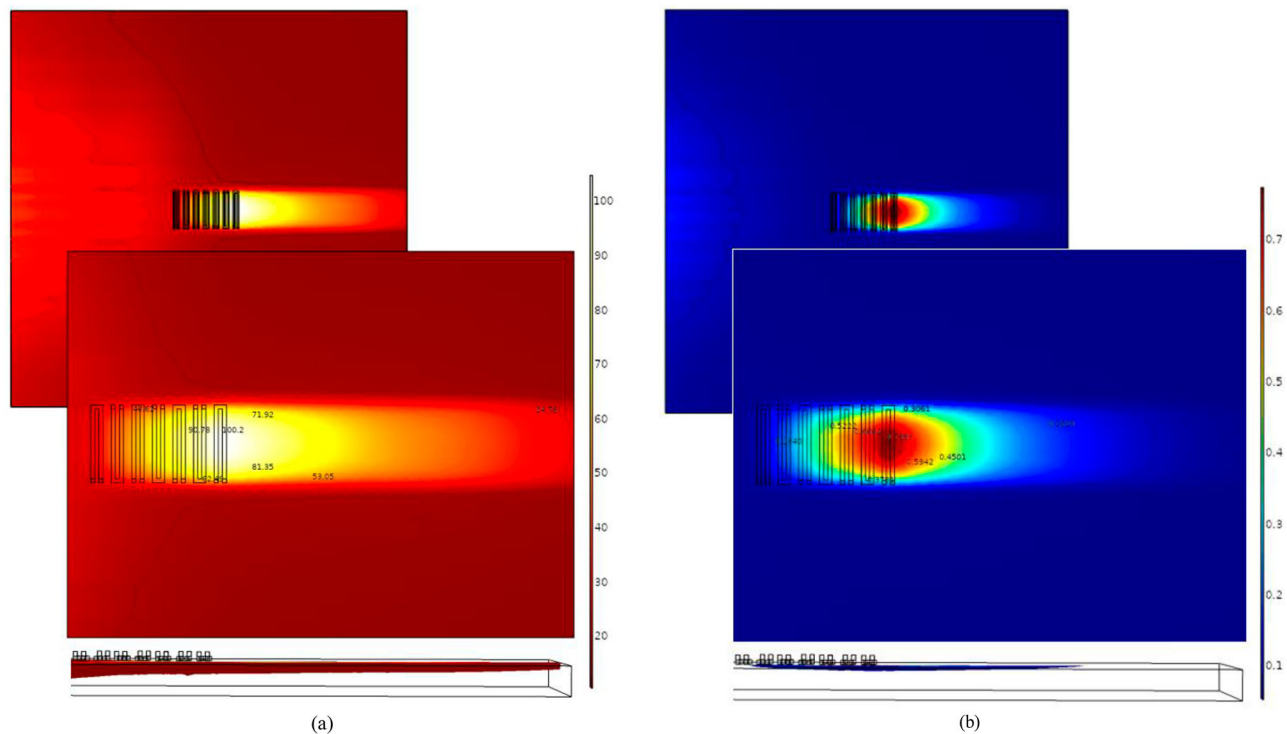
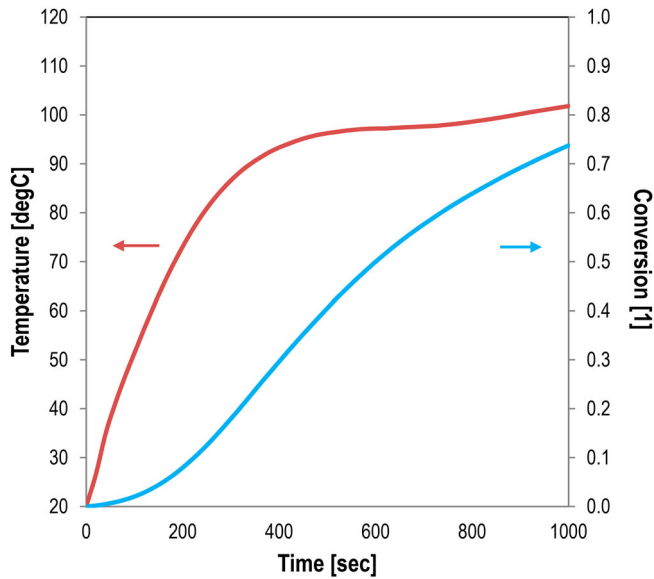


Figure 5. Gradient distribution of (a) temperature and (b) conversion after 1000 sec of electro-magnetic induction in the medium/pavement ( $E_a$ :50 KJ/mol,  $A_f$ : 1000 1/s).

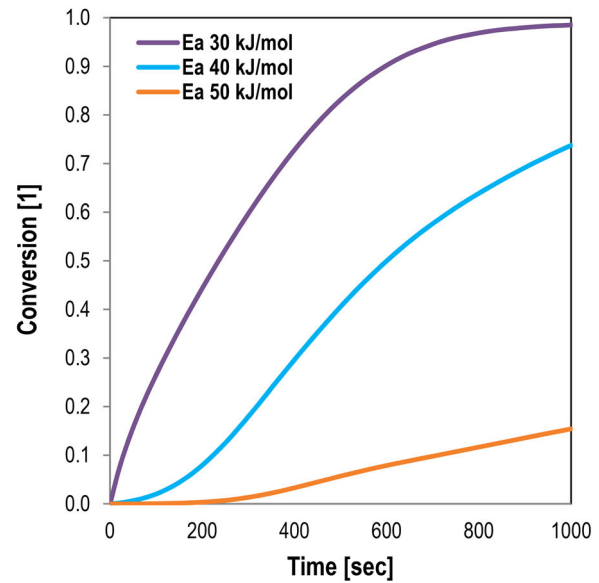


**Figure 6.** Temperature and conversion development in the medium/pavement ( $E_a$ : 50 kJ/mol,  $A_f$ : 1000 1/s).

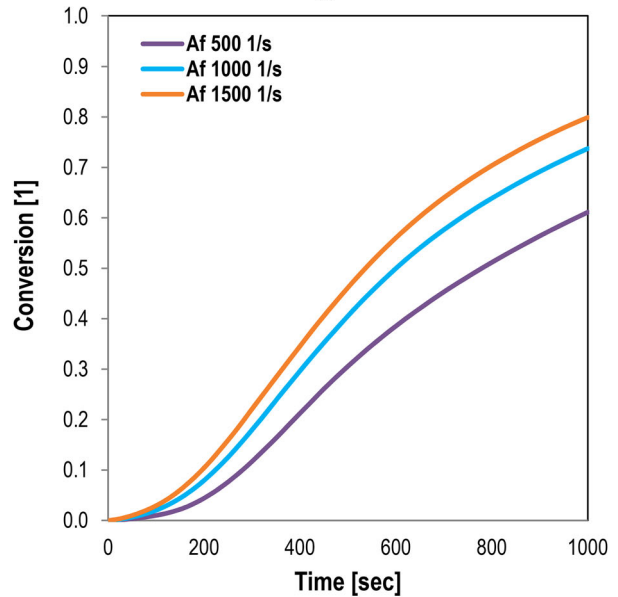
(a–b) shows the predicted distribution via simulation of the temperature and the conversion for the studied medium.

In Figure 6, a typical graph of conversion increase on a surface point of the layer is plotted with the temperature increase generated by a travelling electro-magnetic source of a specific induction configuration. The reaction rate can be tuned by changing either the chemistry (reactivity) of the EA system or the operational conditions of the electro-magnetic source. Faster polymerisation (crosslinking) of EA will be possible when higher heating rates are generated via higher applied power during the in-situ induction heating. Nevertheless, in this study, the focus was on the chemistry-related parameters that govern the polymerisation process of EAs, and in particular the impact of activation energy and reaction rate. These parameters were investigated also elsewhere (Apostolidis *et al.* 2018a), but never in a simulation framework incorporating a moving electro-magnetic source. Therefore, sensitivity analyses were performed to quantify the influence of activation energy ( $E_a$ : 30, 40 and 50 kJ/mol) and reaction rate ( $A_f$ : 500, 1000 and 1500 1/s) on the efficiency of the proposed polymerisation method.

The results of the current multi-physics analyses and especially the predicted conversion (i.e. amount of crosslinks in medium) at the surface of the studied medium over time and along the height of the asphalt layer (0.3 m thickness) are demonstrated in Figures 7 and 8, respectively. According to Figure 7, the conversion increases faster reaching almost the fully cured condition for  $E_a$  30 kJ/mol, in other words for the lower values among the studied scenarios. Higher values of  $E_a$  demand higher levels of applied induction power or slower travelling speeds to obtain a similar conversion on the surface of the medium with a low  $E_a$  value for EAs. During the induction heating-driven polymerisation, the shape of evolution (Figure 7(a)) and the distribution along the height (Figure 8(a)) of the conversion is changing by varying the activation energy of the studied medium. Moreover, the increase of  $A_f$  from 500 to 1000 and to 1500 1/s initiates a slight



(a)



(b)

**Figure 7.** Surface conversion development of medium/pavement during electro-magnetic induction; sensitivity analysis of (a) activation energy ( $A_f$ : 1000 1/s) and (b) reaction rate ( $E_a$ : 50 kJ/mol).

acceleration of the polymerisation process. However, the overall crosslinking performance is mainly influenced by the  $E_a$  which governs the efficiency of polymerisation via induction heating. From a mechanistic point of view, it should be mentioned that every conversion level is related to a certain level of stiffness (Apostolidis *et al.* 2019b). The generated induction heat has a distinct influence on the generation of crosslinks in EA systems even when the electro-magnetic source is moving with a certain travelling speed. The benefit of implementing the induction heating method to cure epoxy-based polymer-modified asphalt mixes is that one can control the heating conditions. The result is that the heat and thus the curing is not only known on the surface of inductive medium but also in-depth. In other words, new crosslinks can be generated by induction not only at the surface of the pavement but also

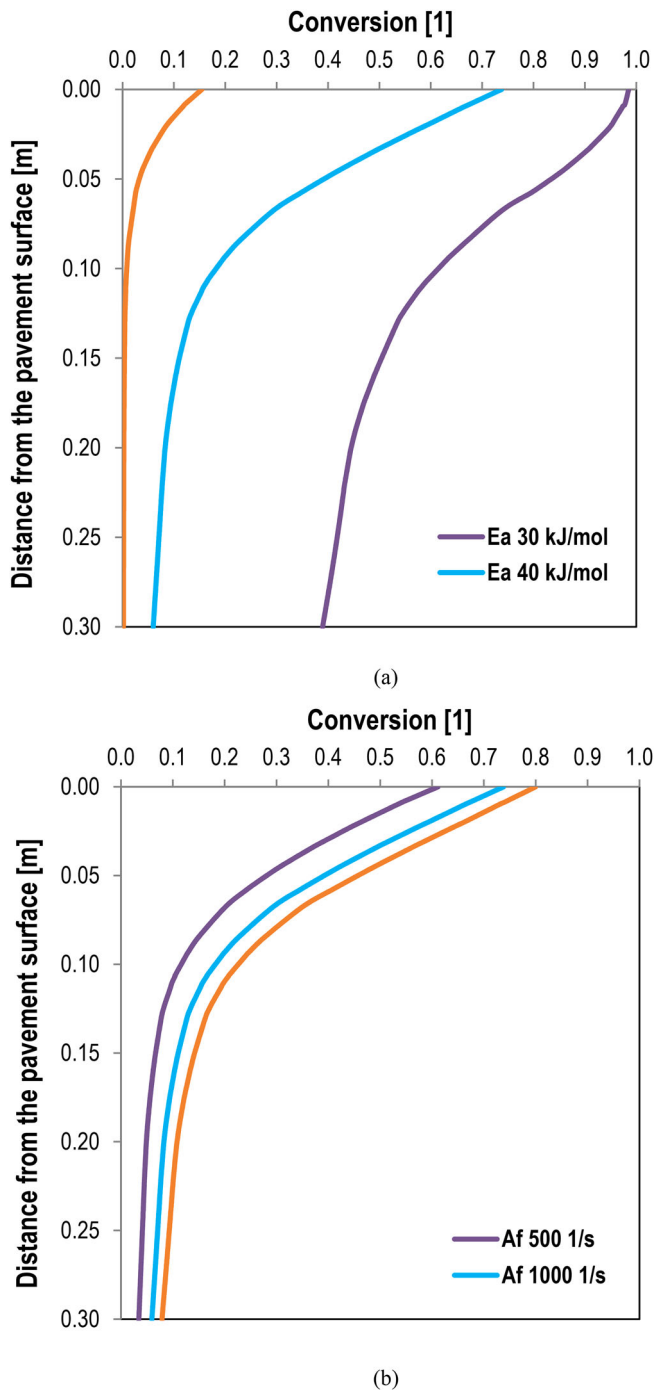


**Figure 8.** In-depth conversion distribution in medium/pavement after 1000 s of electro-magnetic induction; sensitivity analysis of (a) activation energy ( $A_f$ : 1000 1/s) and (b) reaction rate ( $E_a$ : 50 kJ/mol).

over the height of the structure by moving the induction system over the surface and as a consequence, the reactions proceed as wanted.

## Conclusions

The use of electro-magnetic induction technology to drive the curing of materials with thermo-hardening nature, herein EA systems, has been studied in this research. This method is called induction heating-driven polymerisation and it can maintain

most of the advantages of an efficient polymerisation technique while being an environmentally friendly in-situ method that helps curing without the use of extra solvents. Particularly, the electro-magnetic induction is able to stimulate the cross-linking of EA in a controlled way at the right time after the pavement construction to release the structure to service (i.e. traffic). The idea is to have in the field a special vehicle available equipped with an induction coil driving over the surface after paving and/or compaction that can pass to heat up the EA layer and accelerate in this way the material polymerisation process. The induction-driven polymerisation process within the inductive medium/pavement might be performed as a single-pass or multi-pass operation. Finally, the interaction of epoxy molecules with the magnetic field is not considered in this model. Electro-magnetic induction could heat up these molecules directly because of the relaxation of molecular dipoles polarisation along the applied field. Therefore, the mobility of monomers which are involved in the polymerisation may be increased along the applied alternating field and they can react further generating crosslinks faster in areas of limited free volumes. This could provide a new function of this technology in crosslinking EAs and could speed up the polymerisation even more and should be considered for future research.

## Disclosure statement

No potential conflict of interest was reported by the authors.

## ORCID

Panos Apostolidis  <http://orcid.org/0000-0001-5635-4391>

Sandra Erkens  <http://orcid.org/0000-0002-2465-7643>

## References

- Apostolidis, P., et al., 2016. Advanced evaluation of asphalt mortar for induction heating purposes. *Construction and Building Materials*, 126, 9–25.
- Apostolidis, P., et al., 2017. Toward the design of an induction heating system for asphalt pavements with the finite element method. *Transportation Research Record: Journal of the Transportation Research Board*, 2633, 136–146.
- Apostolidis, P., et al., 2018a. Chemo-rheological study of hardening of epoxy modified bituminous binders with the finite element method. *Transportation Research Record: Journal of the Transportation Research Board*, 2672, 190–199.
- Apostolidis, P., 2018b. Induction healing of asphalt mixes with steel slag. In: E. Masad et al., ed. *International conference on advances in materials and pavement performance prediction*. TRB.
- Apostolidis, P., et al., 2019a. Evaluation of epoxy modification in bitumen. *Construction and Building Materials*, 208, 361–368.
- Apostolidis, P., et al., 2019b. Kinetic viscoelasticity of crosslinking epoxy asphalt. *Transportation Research Record: Journal of the Transportation Research Board*. doi:10.1177/0361198119835530.
- ASM International Materials Properties Database Committee, 2000. *ASM ready reference electrical and magnetic properties of metals*. 1st ed. ASM International.
- Balala, B., 1969. Studies leading to choice of epoxy asphalt for pavement on steel orthotropic bridge deck of San Mateo-Hayward bridge. *Highway Research Record*, 287, 12–18.
- Bueno, M., et al., 2018. Induction heating technology for improving compaction of asphalt joints. *International Journal of Pavement Engineering*. doi:10.1080/10298436.2018.1554218.

- Burns, C.D., 1964. *Laboratory and field study of epoxy-asphalt concrete*. Technical Report 3-368, US Army Engineer Waterways Experiment Station, US Corps of Engineers.
- Chen, C., et al., 2018. Performance characteristics of epoxy asphalt paving material for thin orthotropic steel plate. *International Journal of Pavement Engineering*. doi:10.1080/10298436.2018.1481961.
- Garcia, A., et al., 2009. Electrical conductivity of asphalt mortar containing conductive fibers and fillers. *Construction and Building Materials*, 23, 3175–3181.
- Herrington, P. and Alabaster, D., 2008. Epoxy modified open-graded porous asphalt. *Road Materials and Pavement Design*, 9 (3), 481–498.
- Highway Statistics, 2016. *Policy and governmental affairs, office of highway policy information federal highway administration*. Washington, DC: U.S. Department of Transportation, 2018.
- Long-life surfacings for roads: field test results*, 2017. Paris: OECD, International Transport Forum. Research Reports.
- Jia, X., et al., 2014. Investigation of tack coat failure in orthotropic steel bridge deck overlay: survey, analysis, and evaluation. *Transportation Research Record: Journal of the Transportation Research Board*, 2444, 28–37.
- Li, S., et al., 2014. Design, preparation and characterization of novel toughened epoxy asphalt based on a vegetable oil derivative for bridge deck paving. *Royal Society of Chemistry*, 4, 44741–44749.
- Liu, Q., et al., 2013. Induction heating of asphalt mastic for crack control. *Construction and Building Materials*, 41, 345–351.
- Lu, Q. and Bors, J., 2015. Alternate uses of epoxy asphalt on bridge decks and roadways. *Construction and Building Materials*, 78, 18–25.
- Luo, S., et al., 2015. Performance evaluation of epoxy modified open-graded porous asphalt concrete. *Construction and Building Materials*, 76, 97–102.
- Prime, R.B., Michalski, C., and Neag, C.M., 2005. Kinetic analysis of a fast reacting thermoset system. *Thermochimica Acta*, 429, 213–217.
- Simpson, W.C., et al., 1960. Epoxy asphalt concrete for airfield pavements. *Journal of the Air Transport Division, Proceedings of the American Society of Civil Engineer*, 86, 57–71.
- Widyatmoko, I., et al., 2006. Curing characteristics and the performance of epoxy asphalts. *Presented at Tenth International Conference on Asphalt Pavements*. Quebec, Canada.
- Wu, J.P., et al., 2017. Long-term durability of epoxy-modified open-graded porous asphalt wearing course. *International Journal of Pavement Engineering*. doi:10.1080/10298436.2017.1366764.
- Yang, L.F., Yao, K.D., and Koh, W., 1999. Kinetics analysis of the curing reaction of fast cure epoxy prepreps. *Journal of Applied Polymer Science*, 73, 1501–1508.
- Yin, H., et al., 2014. Thermal, damping, and mechanical properties of thermosetting epoxy-modified asphalts. *Journal of Thermal Analysis and Calorimetry*, 115, 1073–1080.
- Zhou, C., et al., 2018. Induction heating assisted compaction in porous asphalt pavements: computational study. *Applied Sciences*, 8, 2308.